MEASUREMENTS IN A FLAT PLATE TURBULENT BOUNDARY LAYER

Jens M. Österlund and Arne V. Johansson
Department of Mechanics, Royal Institute of Technology
100 44 Stockholm, SWEDEN

ABSTRACT

An experimental study has been made of flat plate turbulent boundary layers using hot-film and hot-wire techniques. The primary goals of the investigation were to investigate the scaling behavior of a turbulent boundary layer at high Reynolds numbers and especially the structure in the near wall region.

Results are here presented for the mean velocity and Reynolds stresses for Reynolds numbers based on the momentum thickness ranging from 2500 to 27000. The high Re makes it necessary to use very small probes in order to resolve the smallest scales in the turbulence. A large effort has been put into the design and construction of miniaturized hot-wires for this experiment. Measurements of the fluctuating skin-friction were made with the hot-wire on the wall technique and a new surface-micromachined MEMS-type hot-film sensor.

INTRODUCTION

The overall character of a turbulent boundary layer is given by the two disparate inner and outer length scales. The outer length scale is commonly taken as the thickness of the boundary layer δ, and the inner length scale as the viscous length $l^* = \nu/u_\tau$ where $u_\tau = \sqrt{\tau_w/\rho}$ is the friction velocity, τ_w is the skin friction and ρ is the density of the air. In the classical approach dimensional analysis of the dynamic equations with boundary conditions leads to a scaling of the mean velocity profile in the inner and the outer parts of the boundary layer in the form,

$$\frac{\overline{U}}{u_\tau} = f\left(\frac{yu_\tau}{\nu}\right) \tag{1}$$

$$\frac{U_\infty - \overline{U}}{u_\tau} = F\left(\frac{y}{\delta}\right) \tag{2}$$

At sufficiently large Renolds numbers there is an overlap region $\nu/u_\tau \ll y \ll \delta$ where the law of the wall (1) and the defect law (2) simultaneously hold. Matching (1) and (2) gives one of the classical results from turbulence theory, the logarithmic overlap region. In inner variables,

$$\frac{\overline{U}}{u_\tau} = \frac{1}{\kappa}\ln\left(\frac{yu_\tau}{\nu}\right) + A \tag{3}$$

and in outer variables

$$\frac{U_\infty - \overline{U}}{u_\tau} = -\frac{1}{\kappa}\ln\left(\frac{y}{\delta}\right) + B \tag{4}$$

By combining 3 and 4 one obtains the logarithmic skin friction law

$$\frac{U_\infty}{u_\tau} = \frac{1}{\kappa}\ln\left(\frac{\delta u_\tau}{\nu}\right) + A - B \tag{5}$$

Recently several researchers have investigated alternatives to the classical theory (Zagarola and Smits, 1998; George, Knecht and Castilio, 1992).

EXPERIMENTAL PROCEDURES

Flat plate boundary layer set-up

The experiments was carried out in the MTL-wind tunnel at the department of mechanics, KTH, see figure 1. The MTL-wind tunnel is specially designed for turbulence and transition experiments (Johansson, 1992). It is equipped with a cooler and the temperature can be kept within $\pm 0.05\ ^\circ C$ The test section is 7 m long with a cross sectional area of 1 m^2 (1.2 m $\times$ 0.8 m). The top and the bottom

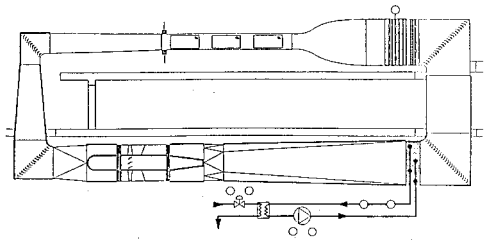

Figure 1: Schematic drawing of the MTL wind-tunnel at KTH

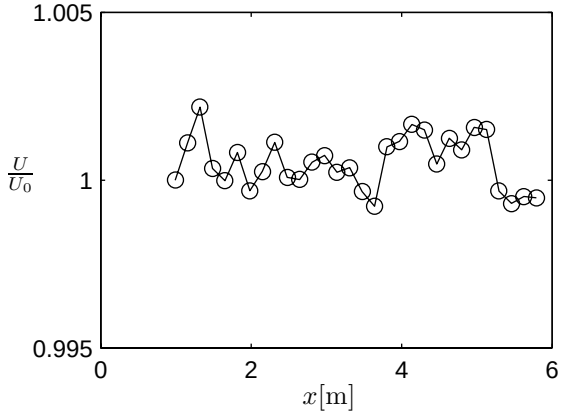

Figure 2: Streamwise mean velocity distribution outside of the boundary layer.

walls are adjustable in order to be able to control the streamwise velocity distribution in the test section. Special care have been taken to reduce acoustic noise and a large part of the return circuit is equipped with noise-absorbing walls. The velocity can be controlled between 0-69 m/s.

A 7 m long flat plate was mounted in the test section. The plate is a sandwich construction of aluminum sheet and aluminum square tubes made in 1 m sections for ease of handling and is resting on two horizontal beams. The leading edge is of elliptical shape with an aspect ratio of 5. Two pressure taps in the elliptical nose are used to position the stagnation point at the centerline of the plate. The positioning of the stagnation point is done by a 2 m long flap mounted at the trailing edge. The alignment of the edges between the plate sections was ensured by the use of cylindric control pins. The step height was measured to be always less than 5 μm. The large scale flatness of the plate was adjusted to within ± 0.5 mm from the horizontal plane.

Zero pressure gradient was achieved by adjusting the upper wall of the tunnel test section. The variation of the velocity outside of the boundary layer was measured by traversing a single hot-wire probe and was less than 0.2%, see figure 2. The boundary layer was tripped by 5 rows of DYMO brand embossing tape letter "V". The two dimensionality of the boundary layer was checked by measuring the spanwise variation of the friction velocity by a Preston tube. The variation was less than $\pm 0.5\%$.

A specially designed traversing system protruding from the plate was used. The vertical relative accuracy is $\pm 1 \mu m$. For the two wire probe measurements a yaw angle traversing system was mounted on top for angular calibrations. The accuracy of that system is $\pm 0.01^\circ$. The traversing system was mounted in one of the plate sections behind the Plexiglas plug where all measurements were taken. The position of the measurement plate section within the whole plate was changed to obtain the following five streamwise measurement positions $x = \{1.5, 2.5, 3.5, 4.5, 5.5\}$ m.

The hot-wires were calibrated in the free stream against a Prandtl-tube immediately before every set of measurements. The calibration was checked after the measurement and if a significant difference occurred the measurement was discarded and the calibration was redone. This happened a few times during the experiments mostly as an effect of dust particles hitting the probe.

Wall distance

The distance from the wall to the probes were measured by a microscope with the tunnel shut off. A laser distance meter mounted under the plexiglas plug and looking directly at the wire made it possible to monitor the wall distance also when the tunnel was running. The error in the absolute wall distance measurements for the single-wire was ± 5 μm and for the X-wire ± 50 μm.

Skin-friction measurements

Since measurement of the mean skin-friction is of primary importance two different methods have been used: oil-film interferometry (Janke, 1994) and fit of measured data to a buffer region mean

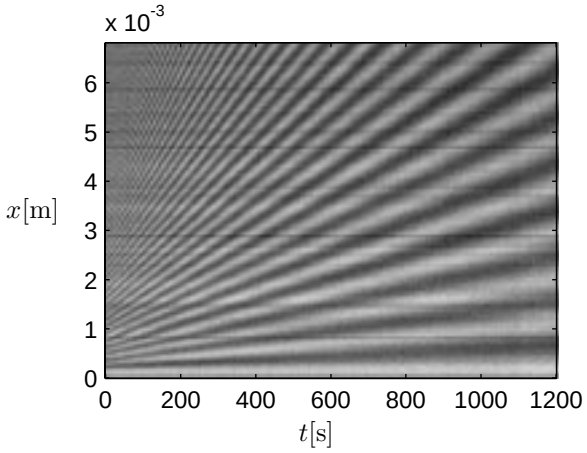

Figure 3: Oil-film interferometry: typical $x-t$ diagram showing the displacement of the interference fringes as an effect of the deformation of the wedge shaped oil-film generated by the shear stress on its upper surface.

velocity profile determined from DNS data.

For the measurements of the fluctuating part of the skin-friction MEMS-type probes were used and also the near-wall hot-wire technique (Fernholz, Janke, Schober, Wagner and Warnack, 1996). The MEMS probe was designed and constructed by Prof. Ho's group at UCLA (Jiang, Tai, Gupta, Goodman, Tung, Huang and Ho, 1996; Ho and Tai, 1998). It was mounted in a cut-out of a printed circuit board (PCB) with all electrical connections on the back except the wire-bonding needed to connect the chip to the PCB. The PCB was itself fitted into a Plexiglas plug that fits into the circular hole at the measurement station. The calibration of the MEMS hot-film and the wall hot-wire was done in the turbulent boundary layer against a Preston tube. The mean skin-friction ranged from 0.3 to 3 times the value of interest in the measurements (Alfredsson, Johansson, Haritonidis and Eckelmann, 1987). A modified Kings law was fitted to the data with a method similar to the one used by Fernholz et al. (1996).

The oil-film interferometry is one of a few independent absolute skin-friction measurement techniques. The deformation of a small droplet of silicon oil, with known viscosity, is recorded in time see figure 3. A video camera was used to record the interference pattern generated when light, from a monochromatic light source, is reflected from the plate surface and from the upper surface of the oil-film. The properties of the silicon oil depend on the temperature, and the cooling system of the tunnel was used to keep the temperature within $\pm 0.1\ ^{\circ}C$.

A new method was also developed to measure the skin-friction by a least squares fit of the measured mean velocity profile to the mean velocity from a direct numerical simulation of a plane Couette flow, in the region $y^+ \in (6, 20)$. The Couette simulation was chosen because we believe it is the DNS that closest resembles the zero pressure gradient boundary layer. For example, the Couette flow has constant total shear across the whole channel and no pressure gradient. The existing boundary layer simulations agree well in the near-wall region with the Couette flow data, but the region of reasonably constant total shear-stress is quite small in the existing low-Reynolds number simulations.

The presence of the wall affects cooling of the hot-wire at close distances to the wall. This effect made us decide the low limit to $y^+ = 6$, no wall-corrections were used. The upper limit should be chosen within a region where the law-of-the-wall can be safely taken to be valid. Here it was chosen to $y^+ = 20$ from the Couette data. The effect of changing the limits was studied and was found to be negligible around the values of the chosen limits. This is a method which is both simple and convenient, and should yield quite accurate results.

RESULTS

Skin friction

Figure 4 shows the skin-friction obtained with the near-wall method, the oil-film method, and from a conventional Clauser fit. The results from the near-wall method and from the Clauser fit are almost inseparable. The data from the oil-film method is slightly lower but still agrees with the former within the experimental uncertainty of the method. The dashed line is the correlation of Fernholz Fernholz (1969).

Mean velocity

Figures 5 and 6 present distributions of the mean streamwise velocity in the boundary layer taken at five streamwise positions and ten free-stream velocities. The profiles were normalized with the friction velocity from the near-wall fit. Both the inner and outer scaling of the profiles collapse rea-

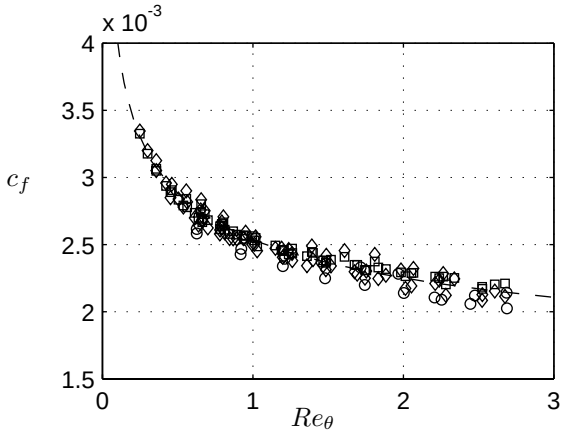

Figure 4: Skin-friction coefficient. ○: oil-film, ◇: hot-wire, □: Clauser-fit, dashed line: correlation by Fernholz (1969).

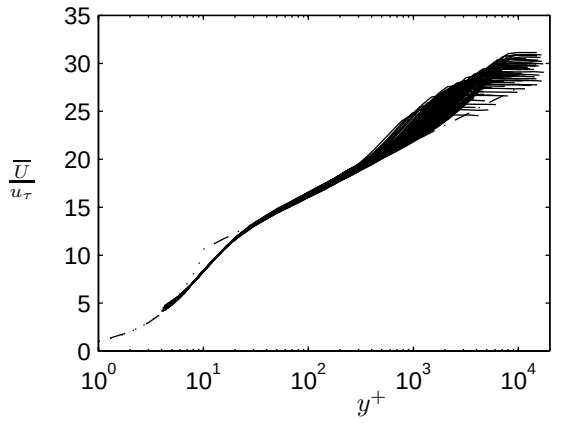

Figure 5: Streamwise mean velocity distribution, inner scaling, $2500 < Re_\theta < 27000$.

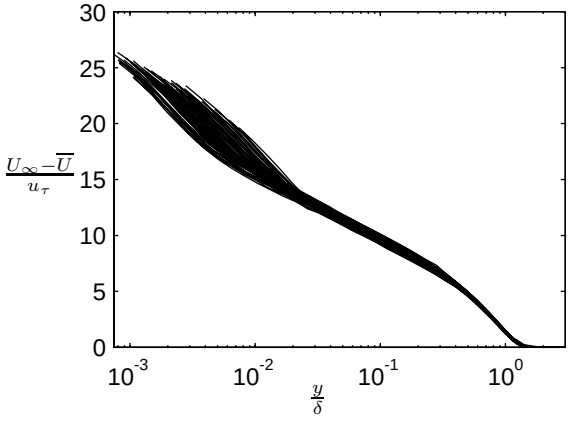

Figure 6: Streamwise mean velocity distribution, outer scaling, $2500 < Re_\theta < 27000$.

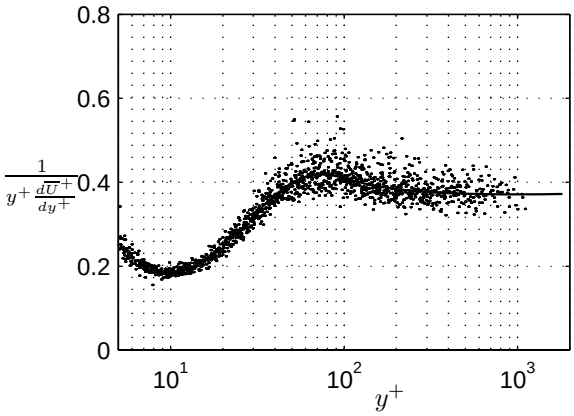

Figure 7: Quantity constant and equal to κ in a log-layer. Only the part of the profiles in which $y/\delta < 0.2$ is shown in inner scaling, $2500 < Re_\theta < 27000$. Solid line is a fit to all data.

sonably well with the classical scaling. From the mean flow profiles it is difficult to draw definite conclusions about the exact functional form in the overlap region and more exact tools are needed.

If a logarithmic region exists the quantity $y^+ d\overline{U}^+/dy^+$ is constant with a value $1/\kappa$ in that region. Figure 7 shows the variation of the reciprocal quantity calculated from the 50 velocity profiles. Only data in which $y/\delta < 0.2$ are shown. Going from the wall and out one can see a slight overshoot before the curves flatten out at around 0.39. The maximum of the overshot is at about $y^+ = 80$ with a value slightly above 0.41. The quantity reaches the constant value for $y^+ > 300$ which indicates a logarithmic overlap region that starts further out than the commonly accepted value of around 50.

If one instead chooses to look at the quantity $(y^+/\overline{U}^+) \cdot d\overline{U}^+/dy^+$ one would see a constant value in a region with a power-law. In figure 8 that quantity is plotted for values of $y/\delta < 0.2$. The curve has a fairly flat part around $y^+ = 100$ with an inflection point indicating behavior close to a power-law locally. Furthermore, it appears to have a slightly decreasing value from $y^+ = 300$ and out, indicating a deviation from the functional dependence of a power-law.

Reynolds stresses

The results from the measurements of the Reynolds stresses with the X- and V-wire probes

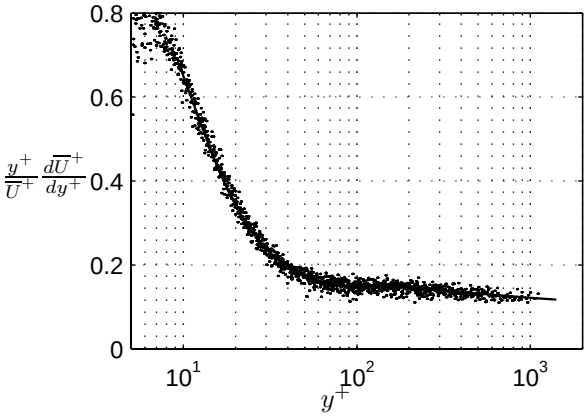

Figure 8: Quantity constant in a region governed by a power-law. Only the part of the profiles in which $y/\delta < 0.2$ is shown in inner scaling, $2500 < Re_\theta < 27000$. Solid line is a fit to all data.

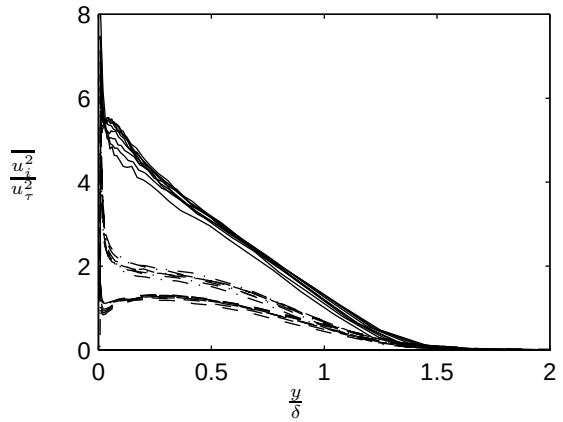

Figure 9: Reynolds normal stress distribution, outer scaling. Solid lines: $\overline{u^2}/u_\tau^2$, dashed: $\overline{v^2}/u_\tau^2$ and dash-dotted: $\overline{w^2}/u_\tau^2$. $6900 < Re_\theta < 22000$.

are shown in figures 9 and 10. Outer scaling gives a reasonable collapse of the data. The profile for the Reynolds shear stress shows a clear Reynolds number variation. The maximum increases and moves outward for increasing Reynolds numbers. The relatively large two-wire probes, compared to the single wire probes, shows an erroneous behavior in the near wall region that is a common problem with these types of probes.

Fluctuating skin friction

Figure 11 shows the results from the fluctuating skin-friction measurements. The results from the near-wall hot-wire and the MEMS-type hot film

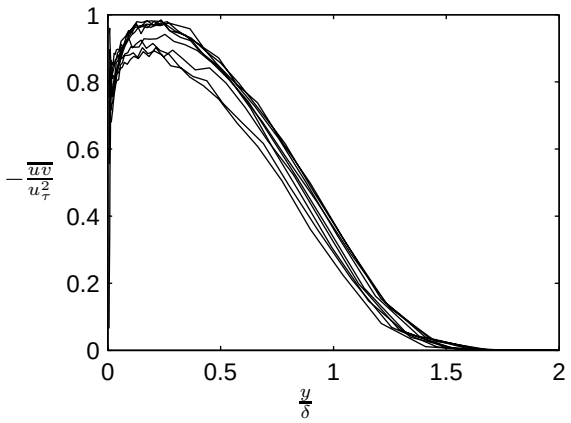

Figure 10: Reynolds shear stress distribution, outer scaling, $6900 < Re_\theta < 22000$. X-probe box side length 220 μm.

are compared with the three measurements from a near-wall hot-wire by Alfredsson et al. (1987). The hot-wire and the hot-film show the same type of behavior. At high Reynolds number there is an almost linear drop in the skin-friction turbulence intensity, that is a result of spatial averaging over the length of the probe. The drop-off at low Reynolds number is not at this point fully understood but we believe that it is caused by thermal coupling to the substrate surrounding the wire or film. At their optimal operation point the maximum turbulence skin-friction intensity is in the range 0.35 to 0.4 which is in accordance with the current state-of-the-art measurements. In spite of the erroneous behavior at low Reynolds number, that it has in common with the wall hot-wire, the MEMS hot-film technique represents a substantial step forward in the field of measuring the fluctuating part of the skin-friction.

BOUNDARY LAYER DATA BASE

Data were recorded, for each position, in one long time series at a rate high enough for spectral studies and sufficiently long for statistical averages. The storage requirements of this procedure is demanding but was conveniently solved by the use of recordable CD-ROM. The advantages are obvious, for example it is always possible to go back and test new data evaluation ideas. The data base contains time series from: single-wire measurements at five different streamwise positions and at ten dif-

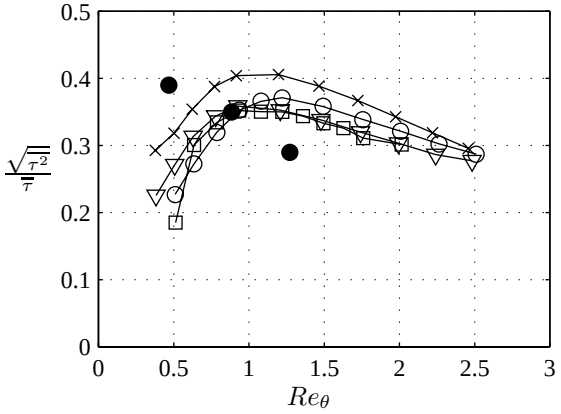

Figure 11: Fluctuating wall shear-stress intensity. ○: wall-wire $l = 500$ μm, □: wall-wire $l = 200$ μm, △: MEMS hot-film $l = 150$ μm, ×: wall-wire $l = 250$ μm, •: wall-wire $l = 750$ μm (Alfredsson et al., 1987).

ferent velocities, X- and V-wire measurements at one streamwise position at eight different velocities, near-wall hot-wire data and two-point data from simultaneous single-wire and MEMS-type hot-film measurements. Evaluation of the large amount of data is, at time of writing, still in progress.

CONCLUDING REMARKS

Basic data on the structure of turbulent boundary layers were presented. The data suggest a log-law starting at about $y^+ = 300$, i.e., the overlap region possibly starts further out than previously assumed. The possibility of a power-law, as suggested by Zagarola and Smits (1998), at least in the region $70 < y^+ < 200$ cannot be ruled out, but must be regarded as a feature of the inner layer and not as a result of a matching of the inner and outer layers. To further clarify the subtle question of the scaling of turbulent wall layers experiments at much larger Reynolds number span is probably the preferable path for future experiments. Also, results from a new MEMS-type hot-film was presented and were found to be in accordance with existing state-of-the-art measurement techniques and DNS-results for the fluctuating skin-friction.

ACKNOWLEDGEMENT

The authors are grateful to Professor Chih-Ming Ho at UCLA for providing the MEMS-type hot-film used in the experiments on fluctuating skin-friction. We wish to thank Mr. Ulf Landen and Mr. Marcus Gällstedt who helped with the manufacturing of the experimental set-up.

REFERENCES

Alfredsson, P. H., Johansson, A. V., Haritonidis, J. H. and Eckelmann, H. (1987). The fluctuation wall-shear stress and the velocity field in the viscous sublayer, *Phys. Fluids A* **31**: 1026–33.

Fernholz, H. H. (1969). Ein halbempirisches Gezetz für die Wandreibung in kompressiblen turbulenten Grenzschichten bei isothermer und adiabater Wand, *ZAMM* **51**: 148–149.

Fernholz, H. H., Janke, G., Schober, M., Wagner, P. M. and Warnack, D. (1996). New developments and applications of skin-friction measuring techniques., *Meas. Sci. Technol.* **7**: 1396–1409.

George, W. K., Knecht, P. and Castilio, L. (1992). The zero-pressure gradient turbulent boundary layer revisited., *Proceedings of the Thirteenth Biennial Symposium on Turbulence*, University of Missouri - Rolla.

Ho, C.-M. and Tai, Y.-C. (1998). Micro-electro-mechanical-systems (mems) and fluid flows., *Ann. Rev. Fluid Mech.* **30**: 579–612.

Janke, G. (1994). *Über die Grundlagen und einige Anwendungen der Ölfilm-interferometrie zur Messung von Wandreibungsfeldern in Luftströmungen.*, PhD thesis, Technische Universität Berlin.

Jiang, F., Tai, Y. C., Gupta, B., Goodman, R., Tung, S., Huang, J. B. and Ho, C. M. (1996). A surface-micromachined shear stress imager, *1996 IEEE Micro Electro Mechanical Systems Workshop (MEMS '96)*, pp. 110–115.

Johansson, A. V. (1992). A low speed wind-tunnel with extreme flow quality - design and tests., *Technical report*, Department of Mechanics, Royal Institute of Technology.

Zagarola, M. V. and Smits, A. J. (1998). A new mean velocity scaling for turbulent boundary layers, *Proceedings of FEDSM'98*.